



TITLE:

# On Vortex Shedding Excitations of Cable-Stayed Bridge of Closed Polygonal Cross Sections

AUTHOR(S):

SHIRAISHI, Naruhito; MATSUMOTO, Masaru

---

CITATION:

SHIRAISHI, Naruhito ...[et al]. On Vortex Shedding Excitations of Cable-Stayed Bridge of Closed Polygonal Cross Sections. *Memoirs of the Faculty of Engineering, Kyoto University* 1976, 38(2): 37-54

ISSUE DATE:

1976-08-31

URL:

<http://hdl.handle.net/2433/280998>

RIGHT:

# On Vortex Shedding Excitations of Cable-Stayed Bridge of Closed Polygonal Cross Sections

By

Naruhito SHIRAISHI\* and Masaru MATSUMOTO\*

(Received December 27, 1975)

## Synopsis

This paper presents a few fundamental instability characteristics of vortex shedding excitations for closed cross sections of bridge structures by means of wind tunnel and water flume tests. Experimental results indicate that the hexagonal form of a cross section with spoilers and flaps is a satisfactory stable cross section for aeolian oscillations. It is also noted that there are multiple synchronized regions of wind velocities for vortex shedding excitations of such cross sections treated here. As far as induced drag forces acting on obstacles and shedding frequencies are concerned, the results by water flume tests well coincide with those by wind tunnel tests.

## 1. Introduction

A number of investigations on the aerodynamic instability of suspension bridges and cable-stayed bridges has been carried out after the failure of the Tacoma Narrows Bridge in 1940. The aerodynamic instability concerning bridge sections is at present classified roughly into coupled flutter, stall flutter, galloping, vortex shedding excitation and buffeting. Although the flutter phenomenon yields to catastrophic oscillations to the structures, comparatively stable cross sections for bridge structures have been proposed as the result of numerous contributions<sup>1)-10)</sup>.

However, as for vortex shedding excitation and buffeting which induce scarcely any catastrophic oscillation but a restricted oscillation with rather small amplitudes, the importance of analysis cannot be overstressed from another aerodynamic point of view. Namely, it is the safety for fatigue failures of structural members and vehicle driving on account of their occurrences at rather low wind velocity. For recently constructed cable-stayed bridges of medium span length, a closed box type of cross sections is frequently adopted from economical

\* Department of Civil Engineering

and esthetic considerations. However, attention should be placed on the aerodynamic stability, especially on the vortex shedding excitation, for the determination of such cross sections. In spite of the fact that numerous studies about the vortex shedding excitations of circular cylinder and other blunt sections have been reported, there remain many problems insufficiently clarified so as to apply such results for bridge sections. This is because of the complicated form of cross sections and the sensibility of field wind depending on environments around such structures.

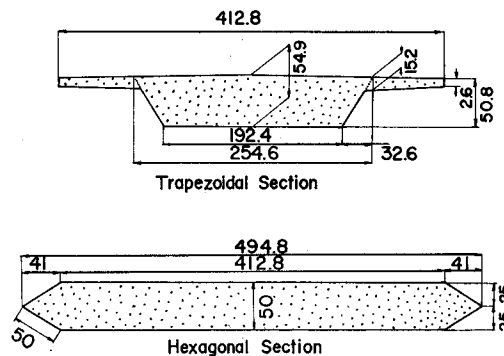
As a representative investigation in this field, C. Scruton<sup>5)</sup> proposed a hexagonal form of cross section for the Severn Bridge. Furthermore, improvements have been achieved by providing such attachments as wind noses and flaps to cross sections<sup>11), 12)</sup>.

In this study, the stability of vortex shedding excitation is investigated in connection with the construction plan for the Ajigawa Bridge, a cable stayed bridge with the main span length being 340 m in Osaka, Japan.

## 2. Section Models and Test Arrangements

Two kinds of typical cross sections of bridges are considered in this work, namely trapezoidal and hexagonal sections as illustrated in Fig. 1. In order to provide a variety of structural configurations, flaps, spoilers, central reserve and handrails are attached to the cross sections as indicated as Table 1.

The models of 1 m span length were tested in the low speed wind tunnel of Kyoto University (Department of Civil Engineering) with a working section of 2.5 m width and 1.5 m height. The wind speed is controlled continuously to reach approximately 20 m/sec at the maximum. The section model is suspended vertically and supported by eight coil springs to give bending and torsional flexibilities



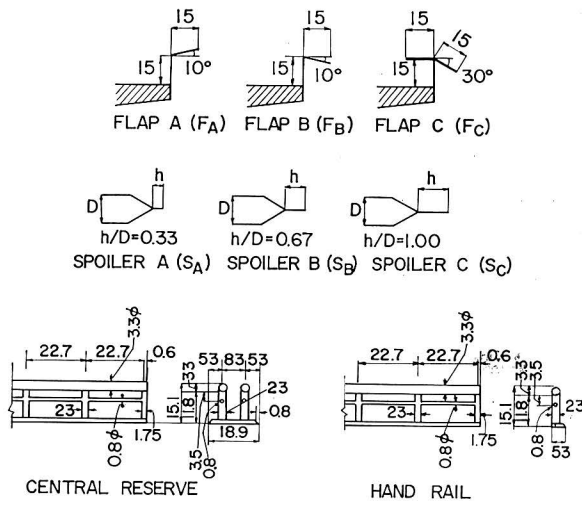


Fig. 1 Dimensions of Models for Wind Tunnel Tests

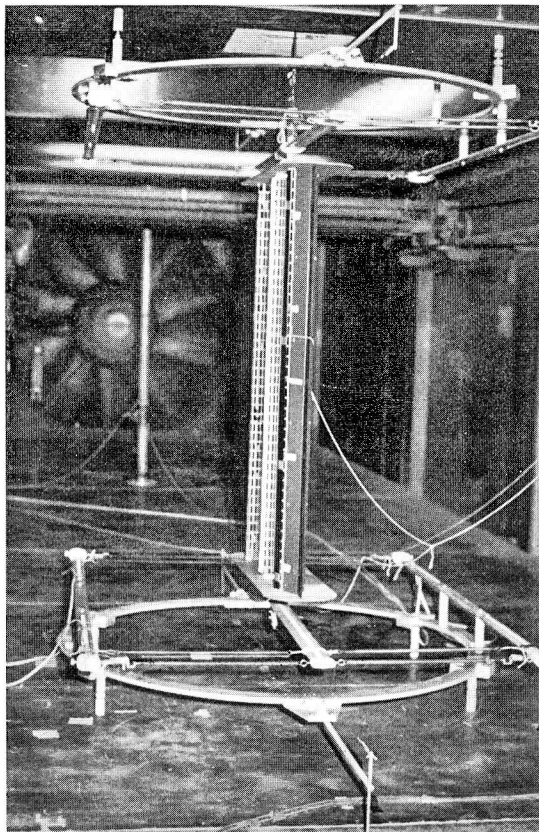


Photo 1 Mounting of Model of Hexagonal Section in Wind Tunnel

as shown in Photo 1. The ratio of bending and torsional natural frequencies is adjusted by the distance between the coil springs. Torsional and bending responses are detected through strain gauges affixed on the  $\square$  shaped pickup placed at the ends of four coil springs. Fluctuating wind velocity in back flow past model is measured by the two directional hot-wire anemometer.

Models with the same geometric shape were used in order to observe the flow pattern around the reposed sections in water flume with a working section of 1 m width and 0.4 m depth. The flow pattern is visualized at the free surface of the water mixed with aluminum powder by driving the model with constant speed.

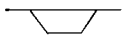

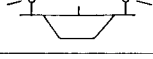
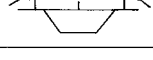
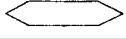
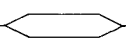
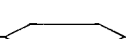
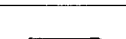
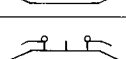
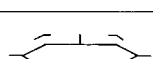
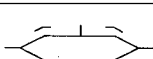
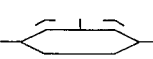
Model	Cross-Section	flap	spoilor	handrail	central reserve
T		—	—	—	—
TF <sub>A</sub>		A	—	○	○
TF <sub>B</sub>		B	—	○	○
TF <sub>C</sub>		C	—	○	○
H		—	—	—	—
H-S <sub>A</sub>		—	A	—	—
H-S <sub>B</sub>		—	B	—	—
H-S <sub>C</sub>		—	C	—	—
$\hat{H}$		C	—	○	○
$\hat{H}F_{cSA}$		C	A	—	○
$\hat{H}F_{cSB}$		C	B	—	○
$\hat{H}F_{cSC}$		C	C	—	○

Table 1 Types of Models

### 3. Aerodynamic Characteristics of Tested Cross Sections

In order to clarify vortex shedding excitation of bridge cross sections, wind tunnel tests are performed to obtain (i) bending and torsional responses of tested models due to vortex shedding at comparatively low wind velocity, (ii) unsteady aerodynamic forces or aerodynamic damping and (iii) vortex shedding frequency in back flow past models. The vibrational characteristics of models for wind tunnel tests are summarized in Table 2. Note that mass-damping parameters for bending oscillation vary from 15 to 40, and those for torsional oscillation vary

Table 2 Vibrational Characteristics of Models in Wind Tunnel Tests

Model	$\alpha$ pitching angle	$m$ mass ( $\frac{kgsec^2}{m^2}$ )	$I$ inertia ( $kgsec^2$ )	$f_\eta$ deflectinal frequency (cps)	$f_\phi$ torsional frequency (cps)	logarithmic decrement		mass parameter	
						$\delta\eta$	$\delta\phi$	$\frac{2m\delta\eta}{\rho D^2}$	$\frac{2I\delta\phi}{\rho D^4}$
$TF_A$	7	0.463	0.0260	4.382	9.904	0.0113	0.0039	34.42	266.79
	5	0.429	0.0269	4.391	9.896	0.0081	0.0058	23.03	413.64
	3	0.463	0.0270	4.382	9.886	0.0113	0.0032	34.08	255.15
	0	0.470	0.0261	4.376	9.918	0.0098	0.0072	29.93	488.50
	-5	0.494	0.0262	4.367	9.994	0.0056	0.0036	18.13	247.19
$TF_B$	7	0.452	0.0273	4.376	9.869	0.0052	0.0056	15.10	392.94
	5	0.452	0.0273	4.376	9.884	0.0063	0.0065	18.30	456.10
	0	0.457	0.0266	4.373	9.884	0.0063	0.0054	18.08	420.92
	-5	0.500	0.0279	4.363	9.850	0.0106	0.0096	34.42	695.69
$TF_O$	5	0.538	0.0264	4.298	9.772	0.0049	0.0046	17.26	318.01
	0	0.589	0.0277	4.289	9.772	0.0090	0.0039	34.70	282.89
	-5	0.589	0.0277	4.292	9.772	0.0049	0.0042	18.91	304.90
$H-S_A$	7	0.606	0.0321	4.138	9.091	0.0071	0.0051	27.41	417.10
$H-S_B$	7	0.602	0.0328	4.116	9.072	0.0073	0.0064	28.31	540.86
	0	0.581	0.0350	4.110	9.058	0.0074	0.0044	26.75	383.20
$H-S_C$	7	0.622	0.0328	4.079	9.299	0.0093	0.0076	36.84	635.11
	0	0.600	0.0348	4.078	8.973	0.0076	0.0047	28.43	407.94
$HF_{CS_A}$	7	0.643	0.0376	4.040	8.905	0.0069	0.0065	28.08	618.73
	5	0.643	0.0376	4.030	8.922	0.0057	0.0055	23.95	540.65
	0	0.649	0.0374	4.027	8.932	0.0057	0.0046	24.50	455.74
	-5	0.649	0.0374	4.036	8.909	0.0065	0.0051	27.96	505.69
$HF_{OS_B}$	7	0.626	0.0363	4.008	8.856	0.0072	0.0048	31.62	457.02
$HF_{OS_O}$	7	0.655	0.0380	3.979	8.785	0.0088	0.0102	36.83	990.67
	0	0.648	0.0364	3.994	8.780	0.0081	0.0092	33.54	911.74

from 250 to 1,000. However, the values of mass-damping parameters are different if one uses the chord length as the representative length. These remain approximately the same for this case.

### 3.1 Bending and torsional responses

Bending and torsional response curves for tested cases are illustrated in Figs 2 to 5. In these figures, the solid line indicates the allowable restricted amplitude for vortex induced excitation, specified by the wind resistant design specification for the Ajigawa Bridge by the Hanshin Express Highway Corporation.

For the model  $TF_A$ , no vortex shedding excitation is generated for the angle of attack  $-5^\circ$  and  $0^\circ$ , but bending amplitudes increase as the positive angle of

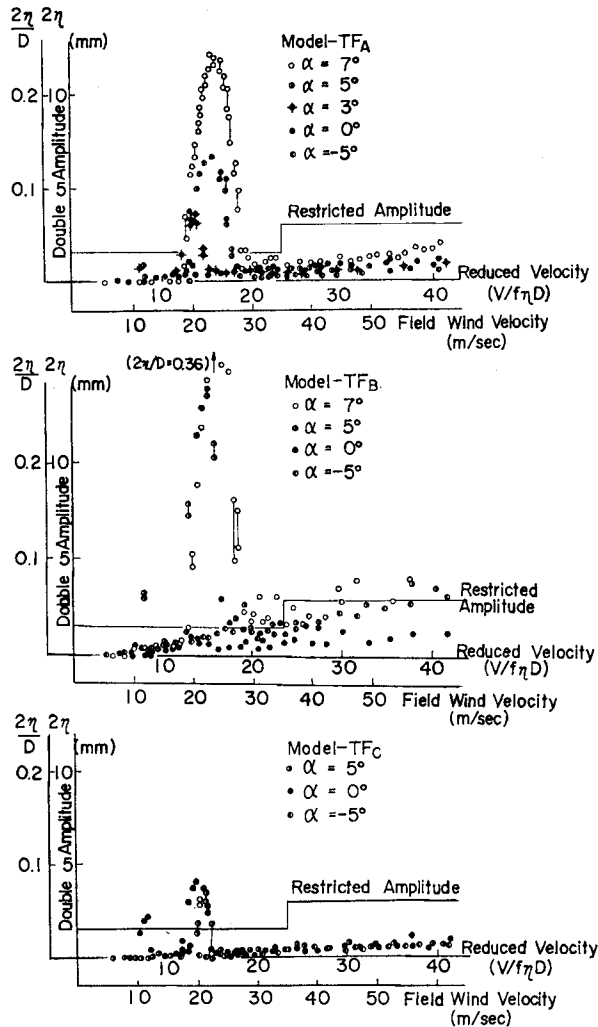


Fig. 2 Deflectional Responses of Trapezoidal Section with Flaps

attack increases as  $3^\circ$ ,  $5^\circ$  and  $7^\circ$ . The critical reduced velocity ( $V/f_p D$ ), at which the maximum bending amplitude is observed, differs slightly as 13.92, 15.85 and 15.83 for angle of attack  $3^\circ$ ,  $5^\circ$  and  $7^\circ$ , respectively. For the positive angle of attack, the two peaks of bending responses are obtained at different velocity regions, for example  $V^*=7.88$  and  $V^*=15.85$  at the angle of attack  $5^\circ$ , although the amplitude at the lower critical velocity is much smaller than the amplitude at the higher critical velocity. As the maximum bending amplitude of the model,  $TF_A$  exceeds the restricted level, this type of cross section is considered to be unfavourable for vortex shedding excitation if the mean angle of attack in field wind reaches  $5^\circ$  or more. (see Fig. 2 and Fig. 3)

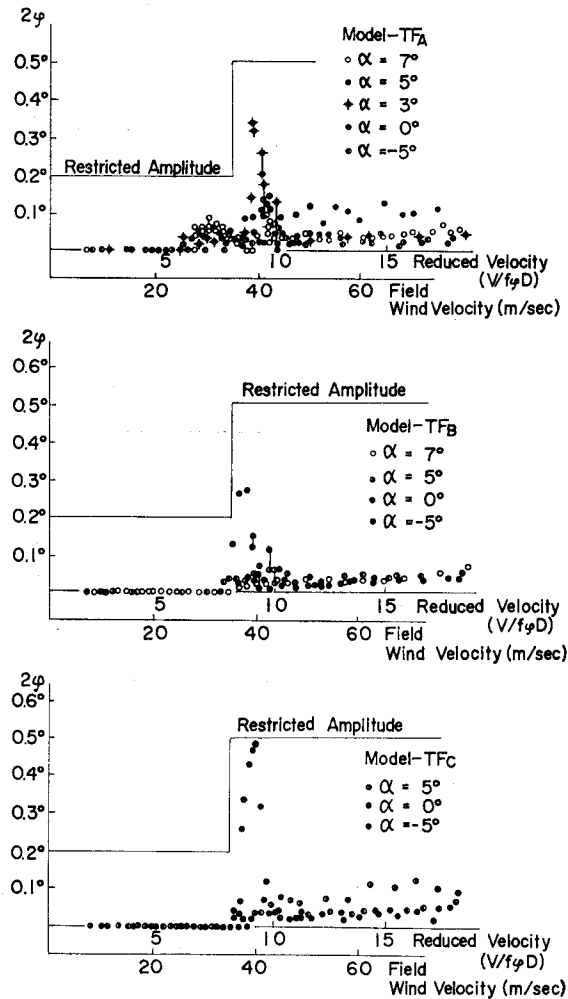


Fig. 3 Torsional Responses of Trapezoidal Section with Flaps



For the model  $TF_B$ , bending and torsional response characteristics are almost similar with those of the model  $TF_A$ . However, the stability for vortex shedding excitation is considered worse than the previous case. (see Fig. 2 and Fig. 3)

For the model  $TF_C$ , the amplitude of bending responses is remarkably reduced so as to compare with previous cases shown in Fig. 2. The torsional excitation is considerably amplified as shown in Fig. 3. It should be noted that the vortex shedding excitation is induced for the model  $TF_C$  at the zero angle of attack, which critical velocity is rather low. For the former cases, induced oscillations occur only when the model receives a certain amount of angle of attack.

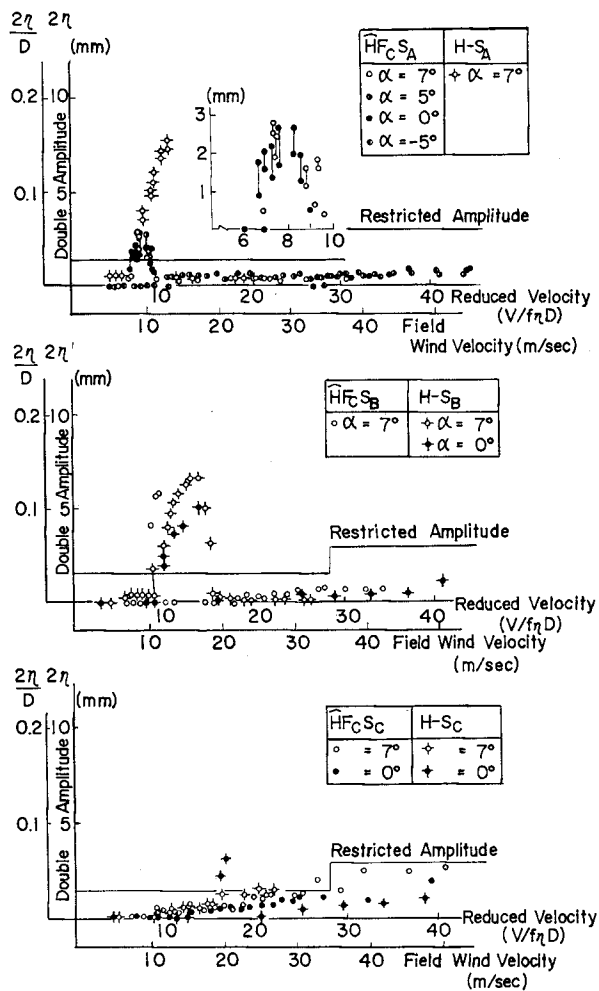


Fig. 4 Deflectional Responses of Hexagonal Section with Three Different Types of Spoilers

For the hexagonal type of cross section and affixture such as a flap is considered to produce noticeable differences in response characteristics of vortex shedding excitation. For example, the bending amplitude of the model  $H-S_A$  is greater than that of the model  $\hat{H}F_C S_A$  as shown in Fig. 4. Torsional response for the model  $\hat{H}F_C S_A$  is hardly obtained, but clearly noticed for the model  $H-S_A$ , as shown in Fig. 5. For the models  $H-S_C$  and  $H F_C S_C$ , the difference is not clearly recognized for bending oscillations, but a noticeable difference exists for torsional responses as shown in Fig. 5. One obtains two different critical reduced velocities for the model  $H-S_B$ , but only one critical reduced velocity for the model  $\hat{H}F_C S_B$ .

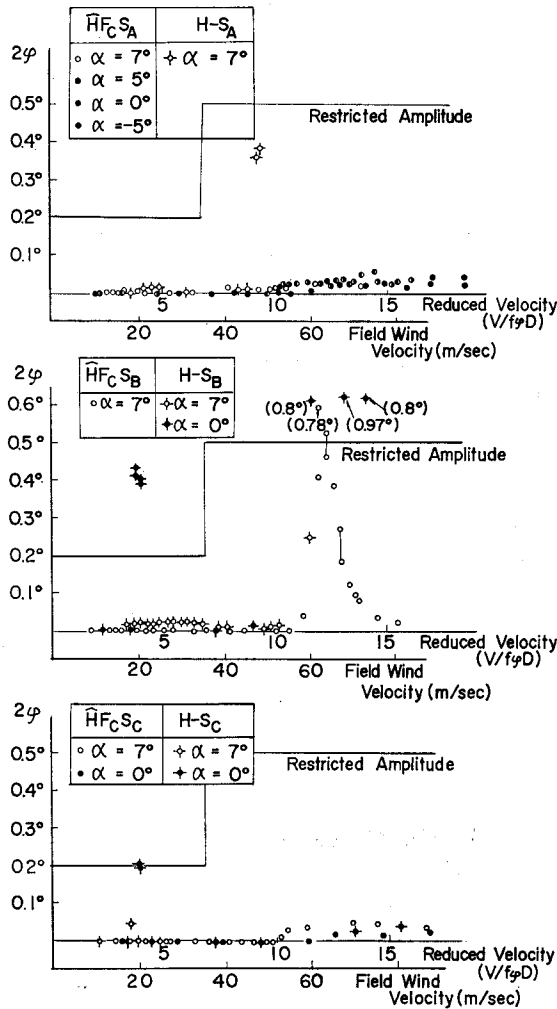


Fig. 5 Torsional Responses of Hexagonal Section with Three Different Types of Spoilers

Since these types of models tend to be excited torsionally by vortex shedding to exceed the restricted amplitude, it can be said that this section with the spoiler B is aerodynamically unsuitable. For the model H-Sc, a comparably small amount of amplitudes is induced deflectionally and torsionally. For the model HF<sub>c</sub>Sc, the vortex shedding excitation hardly generates bending and torsional responses, as shown in Figs 4 and 5.

Through this wind tunnel test a few important characteristics for the vortex shedding excitation are obtained. The angle of attack is an important influential parameter for the vortex shedding excitation, and the instability in deflectional responses tends to increase with the angle of attack. Moreover, strong torsional instability tends to occur at the small angle of attack. Such affixtures as flaps and spoilers to the two kinds of basic cross sections considered here do not always give stabilizing effects on vortex shedding excitation. Also, note that the optimum shape, size and location of affixtures may vary delicately with the basic cross section. Two or more different critical reduced velocities at which vortex induced oscillations occur, may or may not exist, depending on the structural configurations of the cross section, which indicates the complexity of the synchronization mechanism.

### 3.2 Unsteady aerodynamic forces

In order to clarify aerodynamic characteristics of structures, a measurement of unsteady aerodynamic forces acting on structures is occasionally performed by means of either the forced vibration method or the free vibration method.<sup>13),14)</sup>

In this work, the unsteady aerodynamic forces in deflectional oscillations are measured by using the free vibration method. The equation for the deflectional oscillation is generally written as

$$m\ddot{y} + c\dot{y} + ky = L_s\ddot{y} + L_y\dot{y} + L_x y \quad (1)$$

In the above equation, the aerodynamic coefficients  $L_s$  and  $L_y$  are neglected to compare with the effects due to the coefficient  $L_x$ . Thus, the non-dimensional aerodynamic coefficient  $k_a$  instead of  $L_x$  is frequently used.

$$k_a = 2m(\delta - \delta_0) / \rho D^2 \quad (2)$$

Figs 6 and 7 indicate variations of the non-dimensional coefficient  $k_a$  of trapezoidal and hexagonal cross sections, respectively, when then the non-dimensional amplitude ( $2\eta/D$ ) is equal to 0.02.

Generally speaking, the angle of attack is remarkably influential on the parameter  $k_a$ , associated with the trapezoidal section to compare with the case of the hexagonal section. In some cases,  $k_a$  becomes negative at two different velocity regions, which indicates the existence of a synchronization of vortex shedding and bending oscillation. In Fig. 7, the quasi-steady forces obtained from aerostatic

coefficients are illustrated simultaneously, which are far different from the unsteady forces in such a low reduced velocity region.

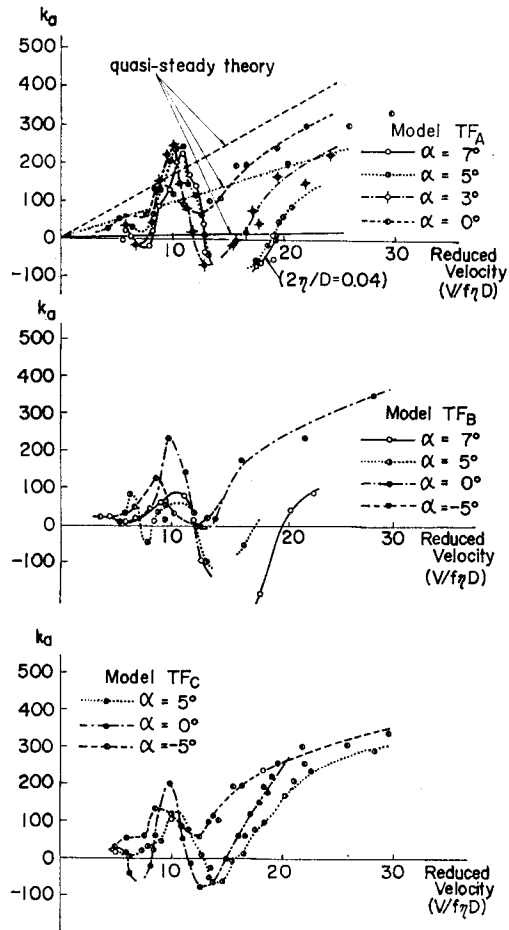


Fig. 6 Aerodynamic Damping Parameter of Trapezoidal Section  
(at  $2\eta/D=0.02$ )

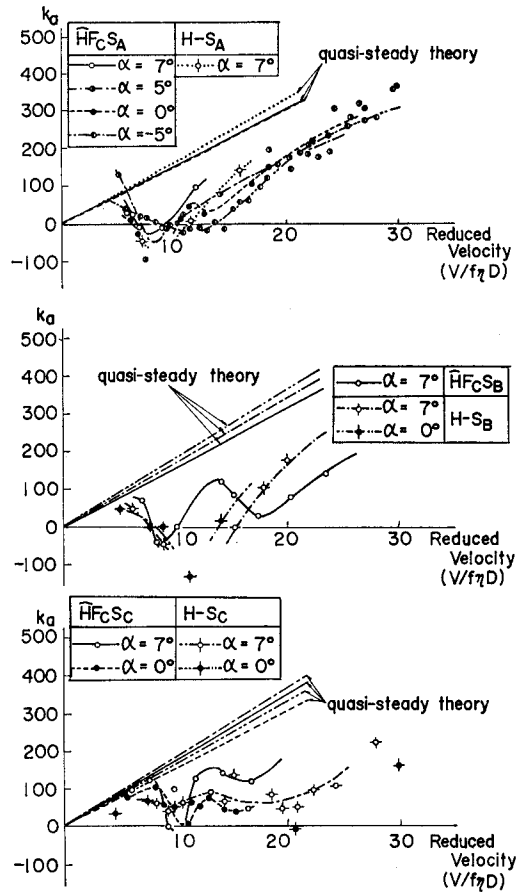


Fig. 7 Aerodynamic Damping Parameter of Hexagonal Section  
(at  $2\eta/D=0.02$ )

### 3.3 Vortex shedding frequency

Since Strouhal's experiment in 1878, strong periodic characteristics in wakes of flow past reposed bluff bodies are widely investigated up to the rather high Reynolds number. Further, fluid-mechanical characteristics in wakes behind oscillating bodies are also investigated for the circular cylinder<sup>15),16)</sup>, for platelike sections<sup>17),18),19)</sup> and for the rectangular section<sup>20)</sup>. As pointed out already, the characteristics of vortex shedding depend considerably on vibrational conditions, namely amplitude and frequency. Thus, it is considered crucial for the aerodynamic analysis of a box type bridge section to examine the interference of wakes with responses and the growth mechanism of generated vortices.

In this work, fluctuating wind velocity in wakes is measured by a hot-wire

anemometer, and the flow pattern past reposed section is examined in water flume described in a subsequent paragraph. Fig. 8 indicates the vortex shedding frequency determined from sharp peaks in power spectrum diagrams, with which the model vibrates as vortex shedding excitation. As far as the frequency characteristics are concerned, the results obtained by use of water flume fairly well agree with those obtained by wind tunnel tests. It is interesting to note that the vortex shedding excitation may occur even if the wind velocity does not coincide with the critical lock-in velocity, where the vortex shedding frequency coincides with either the bending or the torsional natural frequency. As an example, the power spectral density function of a lateral component of wind velocity in wake behind the model H-S<sub>B</sub>, set at zero angle of attack, is illustrated in Fig. 9. This is obtained at the wind velocity 2.05 m/sec and 5.20 m/sec, where typical deflectional and torsional vortex excitations occur. It can be noted that peaks in power spectral density of fluctuating wind velocity in wake behind the model correspond to multiples of natural frequencies and the Strouhal's frequency. The synchronizations at different velocity regions imply that it is insufficient to examine the stability of vortex shedding excitation only at neighbourhood of the critical wind velocity  $U_{cr}$ , where the shedding frequency on the reposed model coincides with its natural frequency. It is necessary to extend to a higher wind velocity region in order to assure the stability for high order synchronization<sup>21), 22)</sup>.

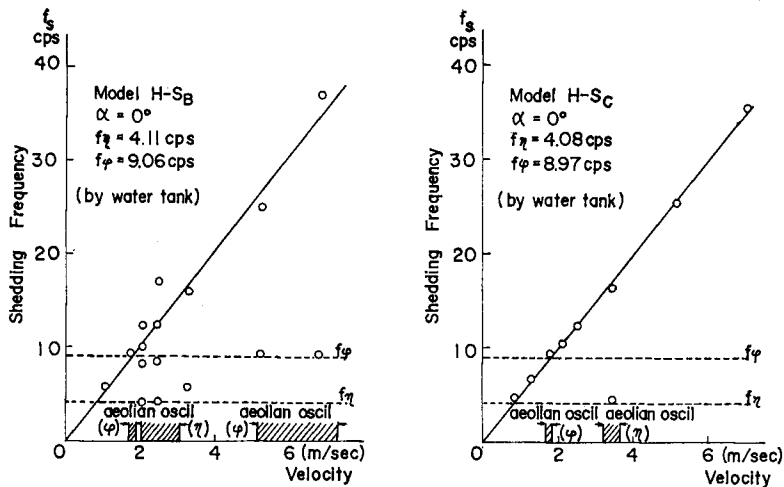


Fig. 8 Comparison of Shedding Frequencies of Hexagonal Section in Wind Tunnel Tests and in Water Flume Tests

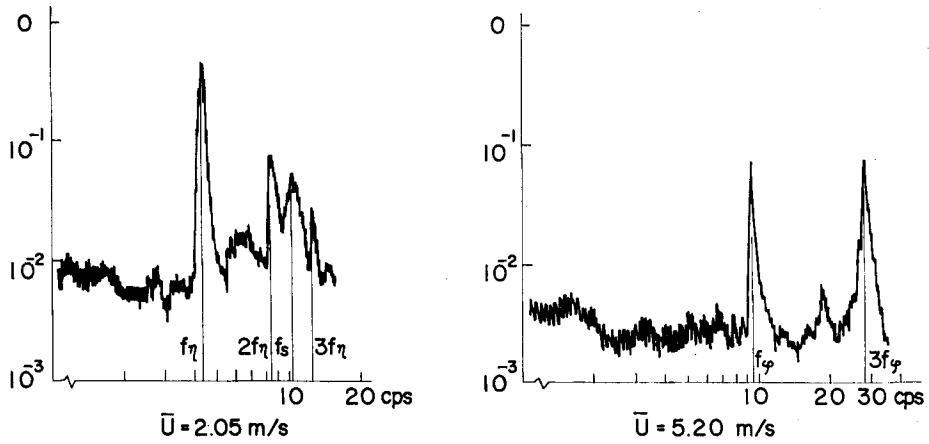


Fig. 9 Power Spectral Characteristics of Chordwise Wind Velocity Components in Back Flow of Model H-S<sub>B</sub>

#### 4. Flow Visualization in Water Flume

As described already, investigations on flow pattern past obstacles have been carried out experimentally as well as theoretically<sup>23)</sup>. A stabilizing condition of vortices was recently proposed by Kronauer<sup>24)</sup> as an extended form of the classical theory of von Karman. Aerodynamic forces induced by vortex shedding are frequently as forcing forces on reposed obstacles, for which the circulatory strength around an obstacle or a periodical lift force has been studied<sup>25), 26), 27), 28)</sup>. There are a number of investigations<sup>15), 16, 20)</sup> that fluid mechanical characteristics of a flow pattern past vibrating obstacles depend on vibrational conditions. Also, synchronization at some different velocity regions is not always determined by the Strouhal number as in previous investigations. It is therefore reasonable to use a dynamic model in which vortex induced forces acting on the vibrating obstacle in the "locking-in" state are assumed as self-controlled forces<sup>29), 30)</sup>.

In order to analyze fluid mechanical characteristics of vortices generated by an obstacle, the flow visualization around the reposed model is carried out in the water flume from which the following physical quantities are obtained: (i) the ratio of induced velocity and mean velocity, (ii) the ratio of longitudinal distance of vortices and depth of model, (iii) the Strouhal number and (iv) the ratio of width of wake and depth of model. By use of these values, the ratio of the lateral distance of the vortex sheet, the depth of the model and the drag coefficient can be determined with the aid of Kronauer's stable conditions;

$$2 \cosh \frac{\pi b}{a} = \left( \frac{V}{v} - 2 \right) \sinh \frac{\pi b}{a} \left( \cosh \frac{\pi b}{a} \sinh \frac{\pi b}{a} - \frac{\pi b}{a} \right) \quad (3)$$

and 
$$C_{DV} = \frac{4}{\pi} \frac{a}{D} \left( \frac{v}{V} \right)^2 \left\{ \coth^2 \frac{\pi b}{a} + \left( \frac{V}{v} - 2 \right) \frac{\pi b}{a} \coth \frac{\pi b}{a} \right\} \quad (4)$$

in which  $v$  = induced velocity  
 $a$  = longitudinal distance of vortices  
 $V$  = mean velocity  
 $Y$  = width of wake  
 $b$  = lateral distance of vortex sheet  
 $D$  = depth of model  
 $C_{DV}$  = drag coefficient

An example of flow pattern past the model  $TF_A$  is shown in Photo 2, and the drag coefficients are shown in Table 3, compared with those obtained from wind tunnel tests.

As long as frequencies of vortices in wake and resulted drag forces are concerned, the results obtained from water flume well agree with those obtained

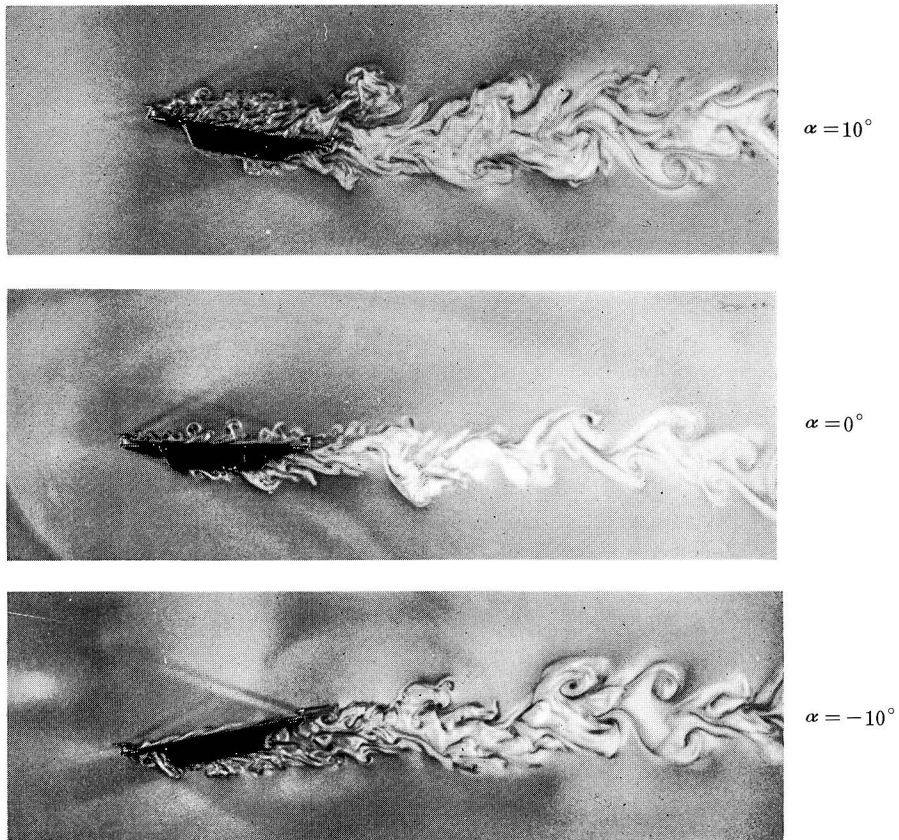


Photo 2 Flow Visualization for Trapezoidal Section  
( $TF_A$ -Model) in Water Flume



Table 3 Comparison of Drag Coefficients

Model $\alpha$ (degree)	$H-S_A$ ( $h/D=0.33$ )			$H-S_B$ ( $h/D=0.67$ )			$H-S_C$ ( $h/D=1.00$ )		
	$C_{D1}$	$C_{D2}$	$\frac{C_{D1}}{C_{D2}}$	$C_{D1}$	$C_{D2}$	$\frac{C_{D1}}{C_{D2}}$	$C_{D1}$	$C_{D2}$	$\frac{C_{D1}}{C_{D2}}$
0	0.678	0.645	1.05	0.699	0.645	1.08	0.631	0.646	0.98
5	0.815	0.759	1.07	0.907	0.750	1.21	0.650	0.794	0.82
10	1.001	1.156	0.87	1.164	1.165	1.00	1.607	1.251	1.31

$C_{D1}$  : drag force coefficient obtained in water flume test

$C_{D2}$  : drag force coefficient obtained in wind tunnel test

from wind tunnel tests. It is rather difficult to distinguish delicate differences in back flows for the different kinds of models by means of flow visualization in water flume, which are aerodynamically recognized in wind tunnel tests.

## 5. Conclusions

Through this study the conclusions are stated as follows:

1. The vortex shedding excitation for flat box sections is an aerodynamic characteristic strongly influenced by the angle of attack of wind, the geometrical shape of basic cross sections and structural affixtures such as spoilers and flaps discussed in this study.
2. Through wind tunnel tests, the hexagonal cross section with spoilers and flaps, namely  $\hat{H}F_cS_c$ , is considered a satisfactory stable section on account of the facts that spoilers and flaps are mutually effective so as to produce a similar pattern of separated flows at the leading edge with one of a thin flat plate and reattachment of separated flows on the deck in an aerodynamically stable state.
3. Attention should be placed on the possibility of an appearance of vortex shedding excitation at more than single critical wind velocity, because the power spectral density function of the fluctuating wind velocity in back flow complies with the multiple of natural frequencies and vortex shedding frequency.
4. The drag coefficients obtained from water flume tests well coincide with those obtained from wind tunnel tests as from 0.8 to 1.3. It is therefore said that flow visualization around the reposed model in water flume is effective to analyze aerostatic characteristics of models.
5. There is no significant difference for induced velocity and longitudinal distance of vortices generated past reposed box sections in spite of the fact that structural configurations are sensitively responsive for the aerodynamic stability of vortex shedding excitation.

It should be noted that further investigations are now called for to know the influence of the turbulence of natural winds, and to clarify growth mechanism of induced vortices past vibrating structures in order to establish a feasible wind design method for bridge structures.

### **Acknowledgements**

The authors wish to express their thanks to Professor Ichiro Konishi for his valuable comments on this work and also to Messers H. Okanan, K. Daimon, H. Takaguchi and Y. Ikemoto for their assistance in the wind tunnel tests and the water flume tests.

### **References**

- 1) F. B. Farquharson; Aerodynamic stability of suspension bridge, Bull. University of Washington, No. 116, Part I, 1950
- 2) C. Scruton; On the wind-excited oscillation of stacks, towers and masts, Int'l Conf. on Wind Effects on Buildings and Structures, NPL, 1963
- 3) F. Bleich; Dynamic instability of truss-stiffened suspension bridge under wind action, Trans. ASCE, Vol. 114, 1949
- 4) A. Selberg; Aerodynamic effects on suspension bridges, Int'l Conf. on Wind Effects on Buildings and Structures, Paper 11 NPL, 1963
- 5) R. H. Scanlan & Ali Sabzevari; Suspension bridge flutter revisited, ASCE Structural Engineering Conference, Seattle, Washington, 1967
- 6) K. Klöppel und G. Weber; Teilmodelversuche zur Beurteilung des aerodynamischen Verhaltens von Brücken, Der Stahlbau, Heft 3 und 4, 1963
- 7) Ali Sabzevari; Aerodynamic response of suspension bridges to wind gust, Proc. Wind Effects on Buildings and Structures, Tokyo, 1971
- 8) A. Hirai; On the aerodynamic stability of suspension bridge, Trans. JSCE, 1947
- 9) M. Ito and H. Tanaka; The characteristics of aerodynamic forces in self-excited oscillations of bluff structures, Trans. JSCE, No. 168, 1969
- 10) N. Shiraishi; On the fundamental characteristics of classical flutter phenomenon of plate-like structures, Trans. JSCE, No. 186, 1971
- 11) R. L. Wardlaw; Some approaches for improving the aerodynamic stability of bridge road decks, Proc. Third Int'l Conf. on Wind Effects on Buildings and Structures, Tokyo, 1971
- 12) N. Narita et al; On restraining procedure of aeolian oscillation of cable stayed bridge, Annual Conf. JSCE, Vol. 28, 1973
- 13) Th. Theodorsen; General theory of aerodynamic instability and the mechanism of flutter, Rep. No. 496, NACA, 1935
- 14) Th. von Karman and W. R. Sears; Airfoil theory for non-uniform motion, J. Aeron. Sci., Vol. 5, No. 10, 1938
- 15) G. H. Koopman; The vortex wakes of vibrating cylinders at low Reynolds numbers, J. Fluid Mech., Vol. 28, Part 3, 1967
- 16) O. M. Griffin; The unsteady wake of an oscillating cylinder at low Reynolds number, J. Applied Mechanics, 1971
- 17) G. H. Toebes and P. S. Eagleson; Hydroelastic vibrations of flat plates related of trailing edge geometry, J. Basic Eng'g, ASME, 1961
- 18) M. E. Greenway and C. J. Wood; The effects of travelled trailing edge on vortex shedding and vibrations, J. Fluid Mech. Vol. 61, Part 2, 1973

- 19) M. Hino and D. Kaneko; Interaction between an oscillating plate and shedding vortices, Trans. JSCE, No. 193, 1971
- 20) Y. Nakamura and T. Mizota; Measurement of unsteady aerodynamic lifts and wake velocity fluctuations for rectangular prisms oscillating in uniform flow, Proc. 3rd National Sym. on Wind Effects on Structures, Tokyo, 1974
- 21) *ibid* (Ref. 1)
- 22) N. Narita et al; Aerodynamic characteristics of cable stayed bridges, Proc. 3rd National Sym. on Wind Effects on Structures, Tokyo, 1974
- 23) Th. von Karman; Flüssigkeits und Luftwiderstand, Physik, z. 13, 1911
- 24) P. W. Bearman; On vortex street wakes, J. Fluid. Mech., Vol. 28, Part 4, 1967
- 25) Technical Reports on Wind Resistant Design for the Honshu-Shikoku Connecting Bridges, Japan Society for Civil Engineers, 1964
- 26) A. Fage and F. C. Johansen; The structure of vortex sheet, Phil. Mag., Series 7, Vol. 5, No. 28, 1928
- 27) *ibid* (Ref. 25)
- 28) T. Sarpkaya; An analytical study of separated flow about circular cylinders, J. Basic Eng'g, Trans. ASME, 1968
- 29) R. H. Hartlen and I. G. Currie; Lift oscillator model of vortex-induced vibration, J. Eng. Mech., ASCE, EM 5, 1970
- 30) Y. Nakamura; Note on the vortex excitation of structures and the synchronization phenomenon in vortex shedding, Proc. 3rd National Sym. on Wind Effects on Structures, Tokyo, 1974